CENTER FOR SPACE RESEARCH

MASSACHUSETTS INSTITUTE OF TECHNOLOGY

N67-27661

(ACCESSION NUMBER)

50

(PAGES)

CR-84501

(NASA CR OR TMX OR AD NUMBER)

(THRU)

01

(CODE)

25

(CATEGORY)

FACILITY FORM 602

GPO PRICE $ _____

CFSTI PRICE(S) $ _____

Hard copy (HC) _____

Microfiche (MF) _____

ff 653 July 65

ACKNOWLEDGEMENTS

The work of J. E. McCune was supported by the National Aeronautics and Space Administration through the M.I.T. Center for Space Research under Grant No. NsG-496. The work of B. D. Fried was partially supported by the Office of Naval Research (Contract No. NONR-4765 (01)) and by the National Science Foundation (NSF Grant-4454).

One of us (J. E. McCune) wishes to thank the Aiken Computation Laboratory of Harvard University for their hospitality in allowing use of their On-Line console, which is supported by ARPA under Contract No. SD-265. This console and the one at UCLA (partially supported by the National Science Foundation, (NSF Grant-4454) were used for all of the computations. Both are served by the on-line system at the University of California at Santa Barbara, and are made available through the courtesy of Professor Glen Culler, Director of the UCSB Computing Center.

I. Introduction

In the following, the numerical solution of the dispersion relation for a magnetized collisionsless plasma in the case of the "loss-cone instability", is described. The solution[1] is based on the use of certain Cauchy integral theorems, combined with the use of graphical display techniques[2]. The numerical results and graphical display information were obtained with the use of the Culler On-Line Computer System[3].

The work reported here is exploratory in nature; only a very limited range of the relevant parameters occuring in the plasma dispersion relation is studied. Attention is focused on establishing the properties of the unstable modes during transition from the Harris-(single-resonance)-type instability[5] to the multiple-resonance type of Rosenbluth and Post[6] for very short wave lengths. A secondary aim of the study is to provide a further illustration of the utility of the Cauchy-integral root-finding technique. No attempt is made in this preliminary study to distinguish between "convective" and "absolute" instabilities; work on this aspect of the problem is under way.

In Sections II - V, the general mathematical problem and its solution are discussed. In Section VI, the physical problem is formulated,[5,6,7,8,10] and in Sections VII-IX, numerical results are presented.

II. The General Mathematical Problem

The direct solution to the mathematical problem of finding the complex zeros of the equation

$$f(z) = 0 \tag{2.1}$$

where f (z) is a complex (in general, transcendental) function of z analytic in the region of interest, has been discussed in references 1 and 2. For the sake of completeness, we outline briefly the principles on which the solution is based, and add a few points of interest not previously discussed. In particular, it was assumed in Refs. 1 and 2 that the zeros of f (z) are all simple; that this restriction is not necessary will be seen below.

The method of solution of (2.1) is based[1] on well-known consequences of Cauchy's residue theorem (slightly generalized from those given in Ref. 4, for example):

$$\sum_{i=1}^{N} n_i z_i^b - \sum_{j=1}^{P} p_j z_j^b = \frac{1}{2\pi i} \oint_C \frac{z^b f'(z)\,dz}{f(z)} \tag{2.2}$$

$$b = 0, 1, 2, 3, \ldots, < \infty$$

where C is any simple, closed curve of finite length in the z-plane enclosing

N zeroes z_i of order n_i and P poles z_j of order p_j .

The most familiar versions of (2.2) are for b = 0 and b = 1, with f (z) such that only <u>simple</u> zeros and poles of f (z) occur within C:[4]

$$N - P = \frac{1}{2\pi i} \oint_C \frac{f'(z)\,dz}{f(z)} \tag{2.3}$$

$$\sum_{i=1}^{N} z_i - \sum_{j=1}^{P} z_j = \frac{1}{2\pi i} \oint_C \frac{z f'(z)\,dz}{f(z)} \tag{2.4}$$

In writing (2.2) or (2.3), (2.4), we have assumed that f'(z)/f(z) is bounded and continuous on C. (If we accidentally choose a curve which passes through a pole or zero of f (z) we will have found that pole or zero in advance!) We have also assumed that f (z) has no branch points or essential singularities within C.

In many cases of interest, we know in advance that f (z) is analytic in the region we wish to investigate. The case for which this is not so and for which we may wish to find all the isolated zeros and poles in a given region will be discussed in a later paper.

If f (z) is analytic inside C (no poles), equations (2.2) simplify to:

$$\sum_{i=1}^{A} n_i z_i^b = \frac{1}{2\pi i} \oint_C \frac{z^b f'(z)\,dz}{f(z)} = I_b(C) \qquad (2.5)$$

In particular, if we have chosen $\hat{C}$ so as to contain only <u>one</u> zero z_1 of previously unknown order n_1 we have, from b = 0:

$$n_1 = \frac{1}{2\pi i} \oint_{\hat{C}} \frac{f'(z)\,dz}{f(z)} = I_0(\hat{C}) \qquad (2.6)$$

and from b = 1:

$$n_1 z_1 = \frac{1}{2\pi i} \oint_{\hat{C}} \frac{z f'(z)\,dz}{f(z)} = I_1(\hat{C}) \qquad (2.7)$$

Thus, if we can find a curve C surrounding any isolated zero, equations (2.6) and (2.7) constitute explicit formulas for both the order and the position of that zero.

This result implies that no loss of accuracy will occur with this method when two roots merge, - - for example, under variation of parameters in f (z).

The problem of finding the roots of f (z) in a region where f (z) is analytic thus reduces to:

1) determining how many zeros - - and of what order - - are within any initially chosen curve C, and

2) judicially varying C by translating it, shrinking it or changing its shape so as to isolate a given zero.

When this is accomplished (2.6) and (2.7) provide the explicit answer to the problem. Some variations of this procedure are discussed in Section IV.

III. Choice and Variation of the Arc C

As a practical matter, it is sufficient to assume at the beginning of the investigation that one is dealing with simple zeros only. This is because in nearly all cases of interest f(z) will also depend on one or more parameters, A, B, .., and multiple zeros will occur only for special values of these parameters. One must begin with some initial values of A, B, .., and if multiple zeros occur at the beginning of the problem, one will recognize this readily enough (see below) and simply choose new values of A, B, ... One can then determine the location of multiple zeros by observing the merging of simple roots as A, B, .., are varied. The importance of (2.6) and (2.7) is to show that no loss of accuracy need be expected if merging occurs.

The utility of the method suggested in Ref. 1 has been illustrated convincingly in Ref. 2, using the Culler On-Line Computing System[3]. With this system, having chosen a curve C, one may immediately display its map, f(C),

in the $w = f(z)$ plane. This display is tantamount to a "Nyquist diagram" for the curve C. With the initial assumption, justified from a practical standpoint above, that $f(z)$ has only simple zeros within C, one can determine by inspection how many such zeros occur (observation of the winding number). This is the same information, of course, as that in (2.5) for $b = 0$. However, the display of $f(C)$ has the further advantage that with a little experience one can usually judge approximately where the zeros lie relative to C and thus decide readily how best to vary C so as to isolate a particular zero. The value of the zero is then obtained from $I_1(C)$, within the accuracy of the numerical integration of $z\, d(\ln f)/dz$.

Since the basis of this root-finding technique is direct and exact, the actual numerical accuracy is limited by:

1) How many distinct points can be used on the computer to represent the curve C in the z-plane and how far apart the resulting points representing $f(C)$ in the $w = f(z)$ plane are;
2) The numerical technique for differentiation of $f(z)$ or $\ln f(z)$; and
3) The numerical technique for integration over the curve C.

Assessment and refinement of this accuracy is discussed in Section V.

IV. Multiple Roots and Contours Enclosing More Than One Root

It is not always possible to recognize the existence of multiple zeros within C simply by inspection of f (C). However, if multiple zeros are in fact present for a given set of parameters, the basic procedure of varying C so as to try to isolate single zeros (reduce the winding number) will perforce reveal their existence.

On the other hand, it may often be more economical to compute one or two additional integrals, I_2 (C), I_3 (C), ..., for a given C than to vary C and recompute f (C). In this case, one can develop useful rules to detect the presence of multiple zeros.

As an example, suppose the winding number for a given C is 2:

$$I_0 (C) = 2 \tag{4.1}$$

In this case, if the curve C encloses a double zero, then

$$I_2 (C) - \frac{1}{2} I_1^2 (C) = 0 \tag{4.2}$$

On the other hand, if C encloses two simple zeros, z_1 and z_2 , then

$$I_2 (C) - \frac{1}{2} I_1^2 (C) = \frac{1}{2} (z_1 - z_2)^2 \neq 0 \tag{4.3}$$

In the same spirit, it is sometimes convenient to work with a contour C which encircles two simple roots or one simple root and one first-order pole, rather than altering C to make it enclose only a single root. In that case we compute the two integrals I_1 and I_2 (the computing time for this being often a small fraction of that required to compute f(C) for a given C). If C encloses two simple roots, z_1 and z_2(as evidenced by visual inspection of the Nyquist diagram or by finding that $I_0 = 2$), their values are given by

$$z_{1,2} = \frac{1}{2}\left[I_1 \pm \sqrt{2I_2 - (I_1)^2}\right] \tag{4.4}$$

If C encloses one first-order pole and one simple root, the value of the latter is

$$z_1 = \frac{1}{2}\left[I_1 + I_2/I_1\right] \tag{4.5}$$

We note also, that the analytic structure of f is often such that the location of its poles is known exactly. (Examples of this are given in sections VII and VIII). In that case, C may enclose one or two roots plus several such known poles without causing any difficulty. For example, if C encloses a simple root and m known poles $z_{p1}, z_{p2}, \ldots z_{pm}$ then in place of (4.5) we have for the root simply

$$z_1 = I_1 + \sum_{i=1}^{m} z_{pi} \tag{4.6}$$

If C encloses two simple roots and m known poles, the former are given by (4.4) with I_1 replaced by $I_1 + \sum_{i=1}^{m} z_{pi}$ and I_2 replaced by $I_2 + \sum_{i=1}^{m} (z_{pi})^2$.

V. Refinement of Accuracy and Convergence

It was pointed out in Ref. 2 that the present root-finding method allows refinement of the numerical value of any root to essentially any accuracy consistent with the digital capacity of the computer and that the "convergence" is quite rapid. The procedure is illustrated in Ref. 2 and also in this report (Section VIII). The method requires, however, the shrinking of the contour to successively smaller circles with their centers at the previously obtained approximate location of the zero. Any subsequent variation of the parameters A, B, ..., of f (z) usually then causes the root to move rapidly out of the small contour so chosen. A new contour must then be constructed and f (C/A, B, ...) recomputed.

Evidently in practice a compromise procedure would often be desirable whereby one could estimate in advance the accuracy of I_1 ($\hat{C}$) for a given $\hat{C}$ which is still large enough to allow significant movement of the root inside $\hat{C}$ under variation of the parameters. If this accuracy is deemed sufficient one can proceed with confidence to obtain a portion of the approximate locus of the given root as the parameters A, B, ..., are varied, i.e. that portion of the locus within $\hat{C}$.

For this purpose, the integral I_o $(\hat{C})$, i.e., the winding number of f $(\hat{C})$ in the w = f (z) plane, has an additional practical use. Since $\hat{C}$ encloses one simple zero, one knows that the exact value of I_o $(\hat{C})$ must be 1 + i 0. The actual numerical value I_o $(\hat{C})$ obtained from the integration compared with the known true value then gives, in most cases, a fair estimate of the numerical accuracy of I_1 $(\hat{C})$.

If the accuracy appears on this basis to be sufficient, one may decide to proceed to vary A, B, ... with $\hat{C}$ held fixed. If the accuracy appears insufficient, however, we can first try to improve the accuracy by keeping C relatively large but rearranging it more symmetrically with respect to the known approximate position of the root or by some other rearrangement. In subsequent calculations of the root, as A, B, ..., are varied, one can continually monitor I_o $(\hat{C})$ to obtain an idea of the accuracy involved. Thus, although the accuracy of I_o $(\hat{C})$ is by no means an absolute measure of the accuracy of I_1 $(\hat{C})$, it can be a useful guide. Any remaining doubt as to the actual accuracy can always be clarified by refining any given root by the method of Ref. 2.

VI. Physical Problem

We are interested in determining the actual values of

growth rates and frequencies occuring in the so-called "loss-cone instability" of a magnetized collisionsless plasma. Roughly, the "loss-cone instability" refers to a situation where the distribution of electron and ion energies perpendicular to the magnetic field has a maximum away from zero.

The Harris dispersion relation[5] has been analyzed for this case by Rosenbluth and Post[6] and by Dory, Guest and Harris[7] and Guest and Dory[8]. In particular, Rosenbluth and Post analyzed the problem in a very general way under certain fairly extreme approximations[10]. We wish to investigate numerically the meaning of their approximations, and try to establish the nature of the transition into the regime where their approximations apply.

We take as our steady-state distribution functions

$$f_{oj} = \frac{1}{\pi^{1/2}\alpha_{\parallel j}} e^{-v_\parallel^2/\alpha_{\parallel j}^2} \frac{1}{2\pi\alpha_\perp} \delta(v_\perp - \alpha_\perp) \tag{6.1}$$

j = ions, electrons

where the $\alpha_{\parallel j}$ and $\alpha_{\perp j}$ are proportional to the mean particle speeds parallel and perpendicular to the magnetic field. Such distributions represent an extreme case of the "loss-cone instability".[7]

We assume disturbances of this steady state of the type $\propto e^{i\underline{k} \cdot \underline{x} - i\omega t}$. We use the notation $k_{\parallel} \equiv \underline{k} \cdot \underline{B}/|\underline{B}|$ where $\underline{B}$ is the magnetic field, and $\underline{k}_{\perp} \equiv \underline{k} - k_{\parallel} \; \underline{B} / |\underline{B}|$. We also define θ such that

$$k_{\parallel} / k = \cos\theta \; ; \; k = \sqrt{k_{\perp}^2 + k_{\parallel}^2}$$

Following Rosenbluth and Post, we assume that the wave lengths and frequencies of interest are such that

$$\frac{k_{\perp} \alpha_{\perp e}}{\omega_{ce}} \ll 1 \; , \quad \frac{\omega}{k_{\parallel} \alpha_{\parallel e}} \gg 1 \tag{6.2}$$

where ω_{ce} is the electron cyclotron frequency, eB/m_e. Under these conditions, we can neglect electron Landau damping and the higher electron cyclotron harmonics. The Harris dispersion relation then reduces to

$$\frac{\alpha_{\perp i}^2 k^2}{\omega_{pi}^2} = \frac{1}{\delta}\left(\frac{\cos^2\theta}{z^2} - \delta^2 \frac{\sin^2\theta}{z_c^2}\right) + \sum_{n=-\infty}^{\infty} \left\{ J_n^2\left(\frac{\sin\theta}{z_c}\right) Z'\left(\frac{z - n z_c}{|\cos\theta| T_i^{1/2}}\right) T_i^{-1} - 2 T_i^{-1/2} |\tan\theta| n J_n J_n' \left(\frac{\sin\theta}{z_c}\right) Z\left(\frac{z - n z_c}{|\cos\theta| T_i^{1/2}}\right)\right\} \tag{6.3}$$

where Z (w) is the plasma dispersion function[9]

$$Z(w) \equiv \frac{1}{\pi^{1/2}} \int_{-\infty}^{\infty} \frac{e^{-u^2} du}{u - w} \; ; \; \mathrm{Im}(w) > 0 \tag{6.4}$$

ω_{pi} is the ion plasma frequency $(n_0 e^2/\varepsilon_0 m_i)^{1/2}$, and we have introduced the following parameters:

$$\delta = \frac{m_e}{m_i} = \frac{\omega_{ci}}{\omega_{ce}} = \frac{\omega_{pi}^2}{\omega_{pe}^2} \; ; \qquad z = \frac{\omega}{k\alpha_{\perp i}}$$

$$T_i = \alpha_{\parallel i}^2 / \alpha_{\perp i}^2 \qquad ; \qquad z_c = \frac{\omega_{ci}}{k\alpha_{\perp i}}$$

(6.5)

In (6.3), the ion term, (the sum on the right) is still exact for the distributions (6.1). Equation (6.3) is to be compared with Equation (4) of Rosenbluth and Post,[6] in which they have drastically reduced the ion term by further approximations.[10] We wish to investigate these further approximations numerically.

Rosenbluth and Post showed that roots of their approximate version of (6.3) are to be found for real $\underline{k}$ in the region defined by

$$0 < \cos^2\theta \lesssim \delta << 1 \tag{6.6}$$

i.e. for propagation nearly perpendicular to $\underline{B}$, with properties such that ($\underline{k}$ real)

$$\mathcal{I}m(z) \sim \mathcal{R}e(z) \sim \frac{\omega_{pi}}{k\alpha_{\perp i}} \gg \frac{\omega_{ci}}{k\alpha_{\perp i}} \equiv z_c \tag{6.7}$$

$$\omega_{pi} \sim k\alpha_{\perp i}$$

It follows that $(\sin\theta)/z_c \gg 1$. In fact, formally, the Rosenbluth-Post approximation corresponds to taking a particular limit of (6.3) in which $|\underline{B}| \to 0$ in the ion term.[10] Thus,

Rosenbluth and Post predict growth rates >> ω_c for real $\underline{k}$.

If roots of (6.3) are indeed to be found in the regions defined by (6.6) and (6.7) and if T_i is not too large, we may make the replacements for each n

$$\frac{1}{T_i} Z'\left(\frac{z - n z_c}{|\cos\theta| T_i^{1/2}}\right) \longrightarrow \frac{\cos^2\theta}{(z - n z_c)^2} \tag{6.8}$$

$$-|\tan\theta| T_i^{-1/2} Z\left(\frac{z - n z_c}{|\cos\theta| T_i^{1/2}}\right) \longrightarrow \frac{\sin\theta}{z - n z_c} \tag{6.9}$$

based on the asymptotic forms[9] for large $|w|$ of Z (w) and Z' (w) . To be precise, we can make these replacements <u>for each n</u> in the sum in (6.3) so long as

$$\frac{\mathrm{Im}\,(z)}{|\cos\theta| T_i^{1/2}} \gg 1 \tag{6.10}$$

Use of (6.8) and (6.9) is equivalent to the neglect of ion Landau damping. With (6.8) and (6.9), Equation (6.3) reduces to

$$\begin{aligned}\frac{\alpha_{\perp i}^2 k^2}{\omega_{p_i}^2} &= \frac{\cos^2\theta}{\delta z^2} - \frac{\delta \sin^2\theta}{z_c^2} + \sum_{n=-\infty}^{\infty} J_n^2\left(\frac{\sin\theta}{z_c}\right) \frac{\cos^2\theta}{(z - n z_c)^2} \\ &\quad + \sum_{n=-\infty}^{\infty} \sin\theta \; 2n J_n' J_n \left(\frac{\sin\theta}{z_c}\right) \frac{1}{z - n z_c} \qquad (6.11) \\ &\approx \frac{\varepsilon^2}{\delta z^2} + \sum_{n=-\infty}^{\infty} 2n J_n'\left(\frac{1}{z_c}\right) J_n\left(\frac{1}{z_c}\right) \frac{1}{z - n z_c} - \frac{\delta}{z_c^2}\end{aligned}$$

where $\varepsilon = \frac{\pi}{2} - \theta$, and the last approximation follows for the range of angles defined by (6.6). It is this last version of the dispersion relation which we study in the following.

VII. Numerical Analysis

As already noted, the analysis of Rosenbluth and Post implies $\sin\theta/z_c \approx \frac{1}{z_c} \gg 1$. In the following, we investigate the roots of (6.11) for

$$\frac{1}{z_c} = 3, 5, 10 \text{ and } 20. \tag{7.1}$$

Actually, in order to find an instability involving interaction with several ion cyclotron harmonics, one requires $z_c < |\cos\theta| \sim \sqrt{\delta}$, which is not satisfied by any of (7.1). However, the range chosen should illustrate the beginning of transition to the regime of multiple resonance. In the following, we also choose

$$\begin{aligned} 0 &< E \leq 8 \\ 0 &\leq F \leq 1 \end{aligned} \tag{7.2}$$

where

$$\begin{aligned} E &\equiv \frac{k^2 \alpha_{\perp i}^2}{\omega_{pi}^2} + \frac{\delta}{z_c^2} \\ F &\equiv \varepsilon^2/\delta \end{aligned} \tag{7.3}$$

Rosenbluth and Post assumed $E \sim 1$, $F \sim 1$ (see relations

(6.6) and (6.7) above).

With the use of the parameters E and F, our results are valid for any sufficiently small value of δ; for any value of z_c, however, there is a minimum meaningful value of E which depends on δ : $E_{min} = \delta / z_c^2$.

Our problem reduces to that of finding the solutions to

$$G(z) \equiv \sum_{n=-\infty}^{\infty} \frac{L_n(x)}{z - n z_c} + \frac{F}{z^2} - E = 0 \tag{7.4}$$

where $x \equiv \frac{k_\perp \alpha_{\perp i}}{\omega_{ci}} \approx \frac{1}{z_c}$ and

$$L_n(x) \equiv 2n J_n'(x) J_n(x) \tag{7.5}$$

Since $L_0(x) \equiv 0$ and $L_{-n}(x) = -L_n(x)$ we can rewrite (7.4) as

$$\tilde{G}(z) \equiv \sum_{n=1}^{\infty} \frac{2 n z_c L_n(x)}{z^2 - n^2 z_c^2}$$

$$G(z) \equiv \tilde{G}(z) + \frac{F}{z^2} - E = 0 \tag{7.6}$$

As we are interested in instabilities and their growth rates, we need only study G (z) in the upper half z-plane. Clearly G (z) is analytic there; it has poles symmetrically disposed along the real z axis with spacing z_c. These poles, of course, are the result of our approximations

(6.8), (6.9). The actual dispersion function has no poles on the real z axis unless $\cos\theta = 0$.

Although our primary interest is in seeking roots with Im (z) > z_c, Re (z) > z_c, with $\mathcal{E}^2 > 0$, we note that (7.6) also has solutions with Re (z) = 0 for perpendicular propagation[7]. Dory, Guest, and Harris point out that these solutions occur in the bands $2.40 \leq x \leq 3.83$, $5.52 \leq x \leq 7.02$, $8.65 \leq x \leq 10.17$, etc., i.e. in the regions where $x\, J_c(x)\, J_c'(x) > 0$. In the following, we shall determine the values of Im (z) (growth rates) of these "zero-frequency" instabilities for x = 3 as a function of E.

The sum in (7.6) converges more and more slowly as x increases. For x = 5 approximately 8 terms are needed for satisfactory accuracy (1 part in 10^6); for x = 10, 18 terms are required. Since the latter case is the most challenging numerically and corresponds most closely to the Rosenbluth-Post analysis, we reserve illustration of the root-finding method for the cases x = 10 & 20. In the following sub-sections, however, we give a few results for x = 3 and x = 5.

VII. A. $x = 3$

For this case, x is too small to give especially interesting results for the higher-frequency instability. Hence, we confine our attention here to determining the growth rates for the "zero-frequency" instability of Dory, Guest and Harris.[7]

Thus, we put $F = 0$ in $G(z)$ for $x = 3$, $(z_c = 1/3)$. If $0 < E \leq E_{crit}$, where

$$E_{crit} = 2x J_0(x) J_0'(x) \qquad (7.a.1)$$

$$= .5290375 \quad (x = 3)$$

a simple zero of $G(z)$ with $\mathrm{Re}(z) = 0$, $\mathrm{Im}(z) > 0$ appears. Using the method described in sections II, III, and V the values of $\mathrm{Im}(z)$ were determined as a function of E. The results are shown in Fig. 1 and Table 1.

Regarding the higher-frequency instability for $x = 3$ ($\mathrm{Re}(z) \approx 1.2\, z_c$), we found $\mathrm{Im}(z) < z_c$ by the same method. Clearly, for $x = 3$, we are quite far from the Rosenbluth-Post regime.

Notice that the minimum meaningful value of E is $9\delta = .0049$ for $z_c = 1/3$, $\delta = (1837)^{-1}$. The values of

ω_{pi}/ω_{ci} corresponding to each value of E are given by

$$\frac{\omega_{pi}}{\omega_{ci}} = \frac{1}{z_c} \frac{1}{\sqrt{E - \delta z_c^{-2}}} \tag{7.a.2}$$

and the corresponding values of ω_{pe}/ω_{ce} by

$$\frac{\omega_{pe}}{\omega_{ce}} = \sqrt{\delta}\, \frac{\omega_{pi}}{\omega_{ci}} \tag{7.a.3}$$

E	IM(Z)
.5290375	0
.4499998	.8123758- 1
.3999998	.1059347
.35	.1275378
.3	.1476323
.25	.1669966
.2	.1861187
.15	.2053615
.1	.2250305
.5 - 1	.2453975
0	.2666455

Table 1. Values of Im (z) for the "zero-frequency" instability of Reference 7 for x = 3 as a function of E = $k^2 x_{\perp i}^2/\omega_{pi}^2 + \delta z_c^{-2}$. The growth rate at E = .05 corresponds to Im (ω) = $.737\omega_{ci}$.

E_{crit} = .52904. $x \equiv k_\perp \alpha_{\perp i}/\omega_{ci} \approx \frac{1}{z_c}$.

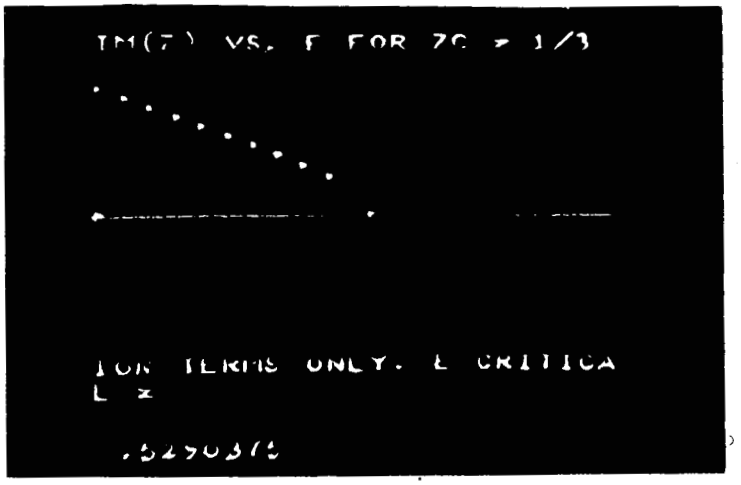

Fig. 1. Plot of Im (z) vs. E corresponding to Table 1. x = 3. F = 0. The minimum meaningful value of E is .0049 for $z_c = 1/3$, $\delta = (1837)^{-1}$.

VII. B. x = 5

In this case the Re (z) = 0 instability does not appear. To determine approximately where the higher-frequency instability appears, we first compute G (z) for real positive z with F = 0 and E = 0. The result is shown in Fig. 2.

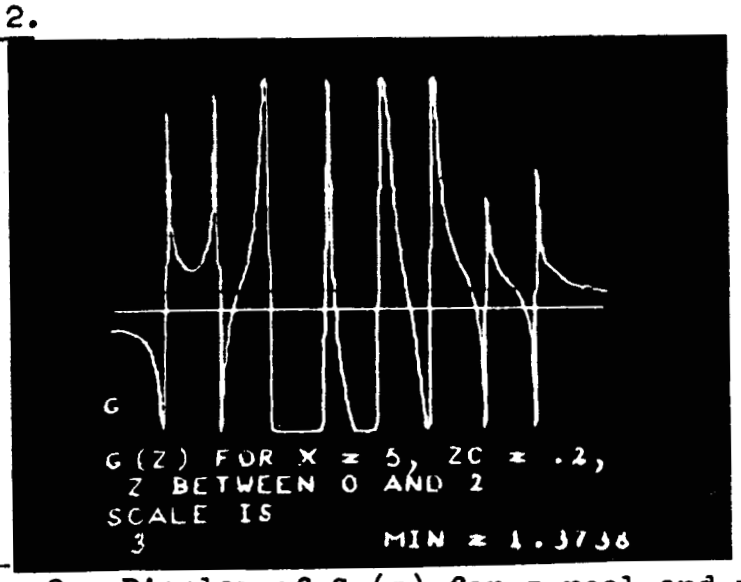

Fig. 2. Display of G (z) for z real and positive, X = 5, F = 0, E = 0. The curve shows a minimum of G for

z between 0.2 and 0.4. This minimum G (= 1.3738) defines E_{crit} for x = 5, F = 0.

Equation (7.6) can be written for F = 0, E > 0

$$\tilde{G}(z) = E \tag{7.b.1}$$

Real solutions of this equation for any E > 0 are thus obtained simply by drawing a horizontal straight line a distance E above the axis in Fig. 2. As E is reduced below the critical value 1.3738 given by the minimum of G between 0.2 and 0.4, two real roots disappear. We expect these to be replaced by two complex conjugate roots. Hence a root should appear in the upper half plane with $0.2 \lesssim \mathrm{Re}\,(z) \lesssim 0.4$ if $E \lesssim E_{crit}$.

The actual values of this unstable root were found by the methods of sections II, III and V. Results are given for F = 0 ($\theta = \pi/2$) over a range of values of E in Table 2. Results for E = 0.6 over a range of values of F are given in Table 3.

1.2
↑
0.6
↑
0
E

.2969668	.365554 - 1
.2947083	.4689159- 1
.2923217	.5633889- 1
.289778	.6544934- 1
.2870114	.7454483- 1
.2839284	.8385667- 1
.280405	.935779 - 1
.2762795	.1038917
.2713384	.114993
.2652876	.1271146
.2577023	.1405606
.2479223	.1557668
.2348251	.1734135

ROOTS FOR H = 90 DEGREES
WITH Z_C = 0.2 AND E =
0(0.1)1.2 E CRIT. = 1.3

Table 2. (Caption on next page).

Table 2. Real and imaginary values of the high frequency root as a function of E for x = 5 and perpendicular propagation ($\varepsilon = 0$). The real parts are given in the left column, the imaginary parts in the right column. The minimum meaningful value of E for x = 5, ($Z_i = \frac{1}{5}$) is $2\delta = .0136$ if $\delta = (18\,\ldots)^{-1}$. The growth rate at $E = 0.1$ corresponds to $Im(\omega) = .778\,\omega_{ci}$ with $Re(\omega) = 1.24\,\omega_{ci}$, and the corresponding value of ω_{pi} is $15.9\,\omega_{ci}$ (Equation (7.a.2).

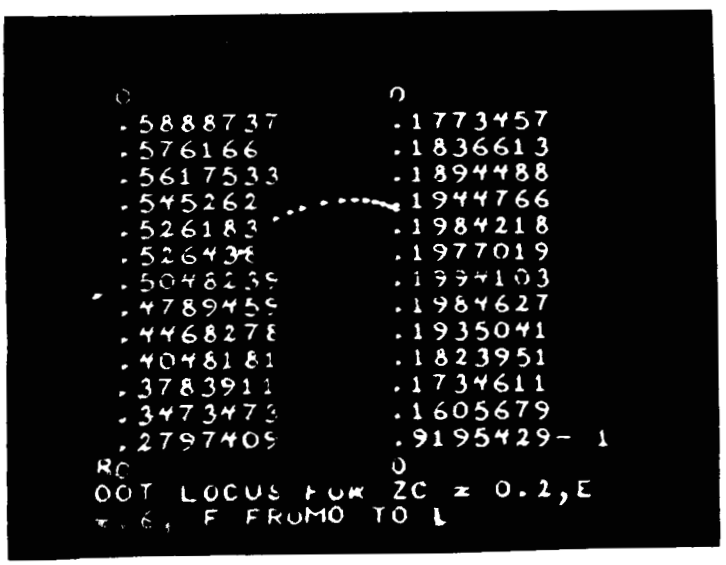

0	0
.5888737	.1773457
.576166	.1836613
.5617533	.1894488
.545262	.1944766
.526183	.1984218
.526438	.1977019
.5046239	.1994103
.4789459	.1984627
.4468278	.1935041
.4048181	.1823951
.3783911	.1734611
.3473473	.1605679
.2797409	.9195429- 1

RO
OOT LOCUS FOR ZC = 0.2,E
= .6, F FROM 0 TO 1

Table 3. Real and imaginary parts of the high frequency root as a function of angle of propagation ($\varepsilon = \pi/2 - \theta$) for x = 5 and E = 0.6. The parameter $F = \varepsilon^2/\delta$ increases upwards in the table: F = 0, .1, .15, .2 (.1) 1.0 . (F = 0.6 is repeated in the table). Results are accurate within about

1%; the roots were not "refined" by the method of Ref. 2 since this assuracy seemed sufficient. The maximum growth rate observed (F = 0.6) corresponds to Im (ω) = $.99\omega_{ci}$. The root locus display is superposed on the table.

We see that also for x = 5 the growth rates remain $\lesssim \omega_{ci}$. As expected, transition to the Rosenbluth-Post regime has not been reached.

On the other hand, if $T_i \approx 1$, $|\cos\theta| \approx \sqrt{\delta}$ we have typically

$$\frac{\mathrm{Im}\, z}{|\cos\theta|\, T_i^{1/2}} \approx 8 \qquad (7.b.2)$$

which is sufficient[9] to allow use of the replacements (6.8) and (6.9) in deriving G(z).

VIII. $x = k_\perp \alpha_{\perp i}/\omega_{ci} = 10$

Because the numerator in the expression for G(z), Eq. (7.6), increases as $n^2 J_n J_n'$, it is necessary to include large values of n when x is large. A more rapidly convergent form is obtained by a simple "subtraction" procedure:

$$\tilde{G}(z) = \frac{4z_c}{z^2}\sum_1^\infty \frac{n^2 J_n J_n'}{z^2-(nz_c)^2} = \frac{4}{z_c z^2}\sum_1^\infty\left[\frac{z^2}{z^2-(nz_c)^2}-1\right] J_n J_n' =$$

$$= \frac{4}{z_c z^2}\left[\frac{J_0 J_0'}{2} + \sum_1^\infty \frac{z^2 J_n J_n'}{z^2-(nz_c)^2}\right. =$$

$$= \frac{2z^2}{z_c}\sum_0^\infty \frac{J_n}{z^2-(nz_c)^2} \qquad (8.2)$$

where

$$K_o = J_o J_o'$$

$$K_n = 2J_n J_n' \quad n \geq 1$$

The numerator now goes as $J_n J_n'$, an improvement by a factor of n^2. In our calculations, we found that truncating the series for G at $n = 15$ give quite adequate accuracy, as is clear from the Tables of K_n and L_n values in the appendix.

VIII.A Critical Values of E

For preliminary orientation, as with $x = 5$, we compute G(z) for real positive z. The result is shown in Figs. 3-6. There are two relative minima in G(z) for $z>0$, one for $0.3<z<0.4$ and a second for $0.6<z<0.7$. These minima correspond to a sign change in $L_n(x)$ from positive to negative as n is increased to $n + 1$. It is easy to check that this occurs only twice for $x=10$ (Appendix I). Figs. 4-6 show these minima more clearly: min [G(z)] = 4.8625 for $0.3<z<0.4$ and min [G(z)] = 7.6798 for $0.6<z<0.7$. (The method for obtaining these values with the On-Line System is discussed in Refs. 2 and 3).

The minimum values of G(z) given above determine the critical values of $E = \left(\frac{k_\perp \alpha_{\perp i}}{\omega_{pi}}\right)^2 + \frac{\delta}{z_c^2}$ for the appearance of two unstable roots with real frequencies $\mathrm{Re}\,(\omega) \approx 3.5\omega_{ci}$ and $\mathrm{Re}\,(\omega) \approx 6.2\omega_{ci}$, respectively, when $\cos\theta = 0$.

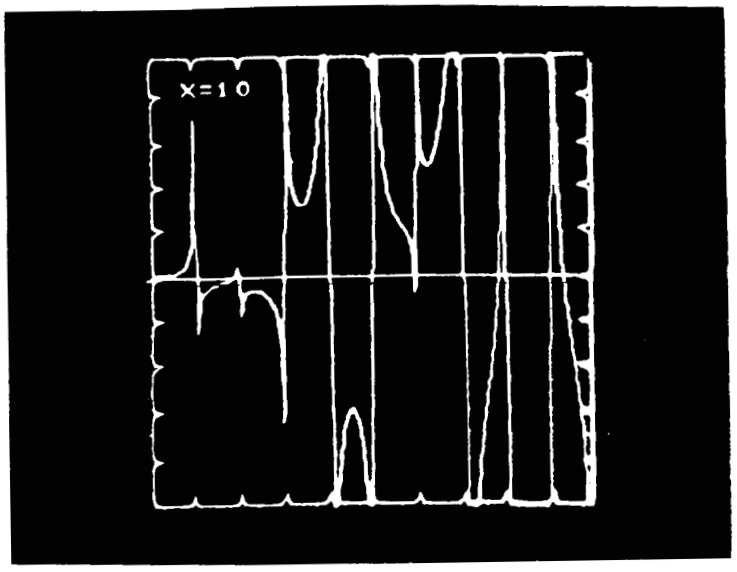

Fig.3 Display of G(z) for x = 10 and positive real z between 0 and 2 . Two relative minima occur, between 0.3 and 0.4 and between 0.6 and 0.7.

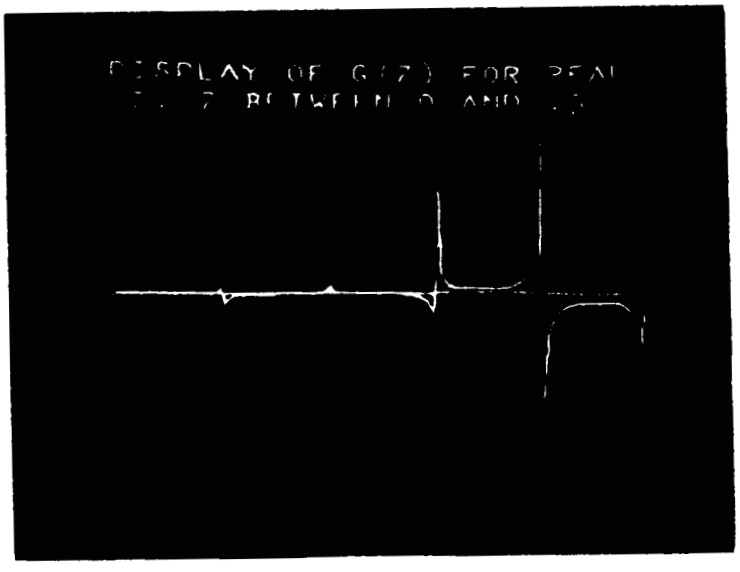

Fig.4 Display of G(z) for x = 10 and positive real z between 0 and .5. The relative minimum between 0.3 and 0.4 is seen more clearly.

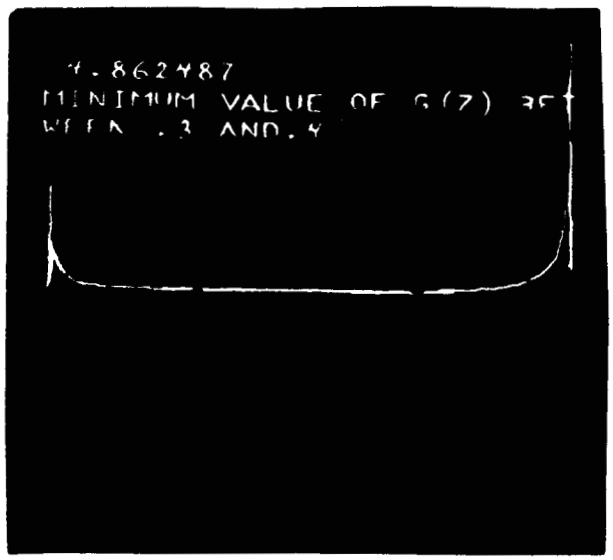

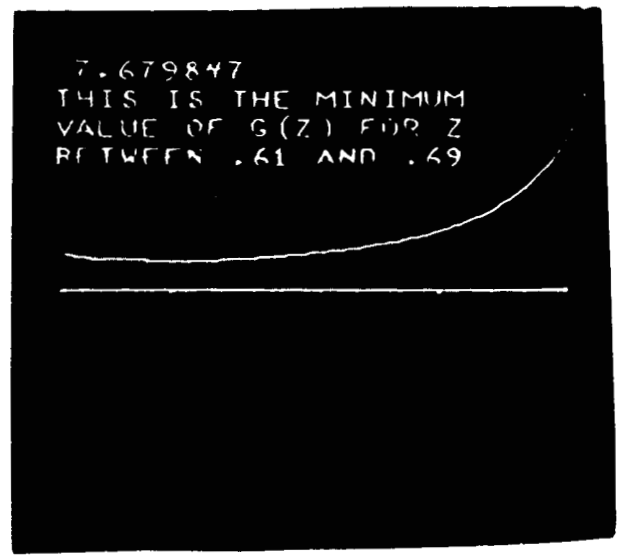

Figs. 5 and 6. The relative minimum values of G (z) between 0.3 and 0.4 and between 0.6 and 0.7, respectively.

In addition to the two unstable roots with positive Re(z) thus identified, there exists a third unstable root for $\cos\theta = 0$ at zero frequency $(\mathrm{Re}(\omega) = 0)$[7]. The critical value of E for this root is[7]

$$E_{crit.} = 2 \times J_0(x)\, J_1(x) = \\ = .21266 \qquad (x = 10) \tag{8.a.1}$$

Thus, for $\cos\theta = 0$, there are $(\mathrm{Re}(z) \geqslant 0)$:

3 unstable roots	$0 \leqslant E < 0.2126$
2 unstable roots	$0.2126 \leqslant E < 4.8625$
1 unstable root	$4.8625 \leqslant E < 7.6798$
0 unstable roots	$E \geqslant 7.6798$

As $\cos\theta$ is increased from zero, the critical values of E are increased because of the F/z^2 term in G (z). Of course, since G (z) is symmetric in Re (z), the unstable roots with positive Re (z) have their images in two further unstable roots with negative Re (z) having the same growth rates.

VIII B. The Rosenbluth-Post Limit

Since the "largest" of the unstable roots strikes the real axis at $z/z_c \approx 6$, we might expect the root values to be given approximately by the Rosenbluth-Post dispersion equation provided Imz turns out to be comparable to Rez. The R-P dispersion equation is obtained from (8.2) by use of the Bessel function identity

$$\sum_{-\infty}^{\infty} J_n(x)\, J_{n-k}(x)\, e^{i(n-k/2)t} = i^k J_k\left[2x \sin(t/2)\right]$$

This allows us to convert the sum in (8.2) to an integral (following essentially the method used by Rosenbluth[10]):

$$\tilde{G}(z) = (2iz/z_c) \int_0^{\infty} dt\, e^{itz} \sin(z_c t/2) \cdot$$
$$\cdot\, J_1\left[2x \sin(z_c t/2)\right] \tag{8.3}$$

While (8.3) and (8.2) are exactly equivalent, we can now introduce the assumption that $\mathrm{Im}\,(z/z_c) \gg 1$, in which case the $\sin(z_c t/2)$ in (8.3) can be replaced by $z_c t/2$ allowing the integral to be evaluated analytically. The result is

$$\tilde{G}(z) \approx \frac{1}{z^2} \frac{1}{(1 - z^{-2})^{3/2}} \tag{8.4}$$

The sign of (8.4) is of crucial importance and can be checked by verifying, directly from (8.2), that $G(z) \to +1/z^2$ as $|z| \to \infty$. Thus, the square root in (8.4) is to be taken as the branch for which $(1 - z^{-2})^{1/2} \to 1$ as $z \to \infty$.

The R-P dispersion relation with our special choice (6.1) for the distribution functions is thus

$$E = \frac{1}{z^2}\left[F + (1 - z^{-2})^{3/2}\right] \tag{8.5}$$

To find the roots of (8.5), it is convenient to define

$$t = -(1 - z^{-2})^{-1/2} \tag{8.6}$$

Then (8.5) takes the form

$$E = (t^2 - 1)(F - t^3)/t^2 \equiv D(t) \tag{8.7}$$

The zeros of D lie at $t = \pm 1$ and at the three cube roots of F (these latter three coalescing to a single root at $t = 0$ when $F = 0$.) By examining a plot of $D(t)$ vs t for real t (Fig. 7), we see that:

a) The root which goes to $t = (-1)$ for $E = 0$ remains real and less than -1 for all E. The inverse of (8.6),

$$z = (1 - t^{-2})^{-1/2} \tag{8.8}$$

gives z real for this branch so it cannot satisfy the condition $\mathrm{Im}\, z \gg z_c$ required for the validity of (8.5). Hence this branch is of no further interest.

b) For $0 < F < 1$, the roots at $t = \sqrt[3]{|F|}$ and $t = 1$ move towards each other along the real t axis as E increases and then go off into the complex t plane, one being the complex conjugate of the other. (We shall call these the <u>right-hand branches</u>.)

c) The roots at $t = \sqrt[3]{|F|}\, e^{\pm 2\pi i/3}$ remain complex as E increases from 0. (We shall call these the left-hand branches.)

For E very large, we see from (8.7) that either $t \to 0$ or $t \to \infty$. In the former case, $t^2 \to -F/E$ so t approaches zero along the positive or negative imaginary axis. In the latter case, $t^3 \to -E$, so t approaches infinity along the lines of argument 60°, 180° or 300°.

To find the actual location of these roots for finite values of

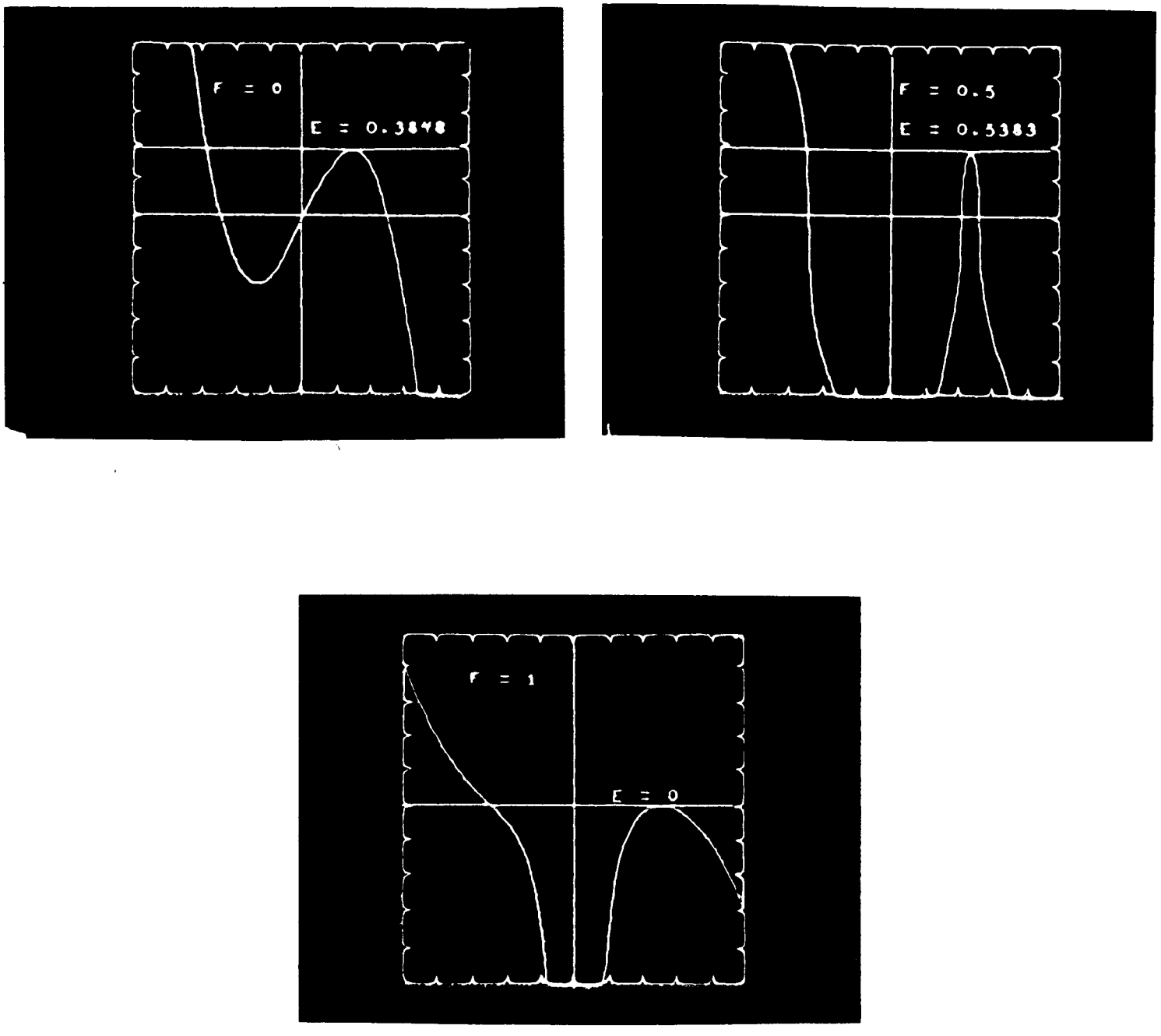

Fig. 7.

Plots of D (t) defined by (8.7) vs t for real t and various values of F. (In the F = 0.5 case, the ordinate is $\sqrt[3]{D}$ rather than D.)

E, i.e., the interpolation between the $E = 0$ and $E \to \infty$ results given above, we simply iterate (8.7) in an appropriate way. For the right-hand branches, we write it in the form

$$(t-1)(t-f) + Et^2\left[(t+1)(t^2+ft+f^2)\right]^{-1} = 0$$

or

$$t^2 + (f+1)t + A = 0$$

where

$$f \equiv \sqrt[3]{|F|} \qquad A(t) \equiv f + t^2 E\left[(t+1)(f^2+tf+t^2)\right]^{-1}$$

Solving this quadratic equation with A treated as "known" leads to the iteration

$$t_{n+1} = \frac{1}{2}\left[-(f+1) \pm \sqrt{(f+1)^2 - 4A(t_n)}\right]$$

which converges very rapidly to the right-hand branches. Similarly, for the left-hand branches we write (8.7) as

$$(\bar{f} - t) - t^2 E\left[(t^2-1)(\bar{f}^2 + t\bar{f} + t^2)\right]^{-1} = 0$$

or

$$t^2 + B(t - \bar{f}) = 0$$

where

$$\bar{f} \equiv f e^{2\pi i/3} \qquad B(t) = (t^2-1)(t^2 + \bar{f}t + \bar{f}^2)/E$$

The iteration resulting from solving this quadratic equation,

$$t_{n+1} = \frac{1}{2}\left[-B \pm \sqrt{B^2 + 4B\bar{f}}\right]$$

likewise converges rapidly, but yields the left-hand branches. The results for $F = 1.0$ are shown in Fig. 8, where the properties previously cited for $E = 0$ (indicated with a heavy dot at the corresponding end of the trajectory) and $E = \infty$ are evident. Note that the two right branches have a common ($E = 0$) starting point at $t = 1$. For smaller values of F, one branch starts at 1, the other at $\sqrt[3]{|F|}$; approach each other along the real axis; and then take

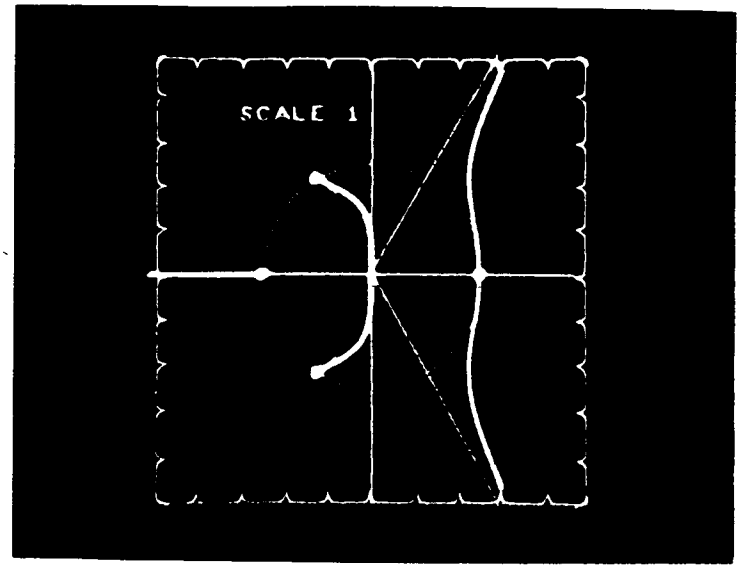

Fig. 8.

Locus in the complex t plane of the roots of E-D (t)=0, with D defined by (8.7). The case F = 1 is illustrated here, with E as a parameter along the curves. The four heavy dots on the unit circle correspond to E = 0, the one at t = 1 being a coalescence of two roots which are distinct when F $\neq$ 1.

off from a point on (0,1) into the complex plane, asymptoting to the 60° lines shown in Fig. 8.

Having found, for given F, root locii for Eq. (8.7) of the sort shown in Fig. 8, it is a simple matter to map the locii back into the z plane using (8.8). On examining these, however, it is found that while the left-hand branches indeed map into solutions of (8.5), the right-hand branches map instead into solutions of (8.5) for the other Riemann sheet, i.e. the one for which $(1-z^{-2})^{-3/2} \longrightarrow (-1)$ as $z \longrightarrow \infty$. In corroboration of this, we show in Fig. 9, for several values of F, the curves in the z plane corresponding to the right-hand branches in the t plane, together with actual solutions obtained from the exact dispersion equation (7.6), <u>but with G(z) replaced by -G(z)</u>. Thus, although the right-hand branches lead to z values for which $\mathrm{Im}\, z \gg z_c$ is magnificently satisfied for $Z_c = 0.1$, they have no bearing on the roots of (7.6). It follows that we must content ourselves with the left-hand branches which, as we shall see, do not yield a very large value of $\mathrm{Im}\, Z/Z_c$.

VIII C. <u>Illustration of the Root-finding Method.</u>

In Fig. 10, we see the z-plane image of one of the "left hand branches" for the case F = 0.5. We choose as initial contour, C, the square shown and compute its image under the mapping

$$z \longrightarrow G(z) = \tilde{G}(z) + F/z^2 - E$$

with E = 2. As shown in Fig. 11, G(C) encloses the origin so C encloses a root of G = 0. To find it, we compute, following (2.7),

(8.9)

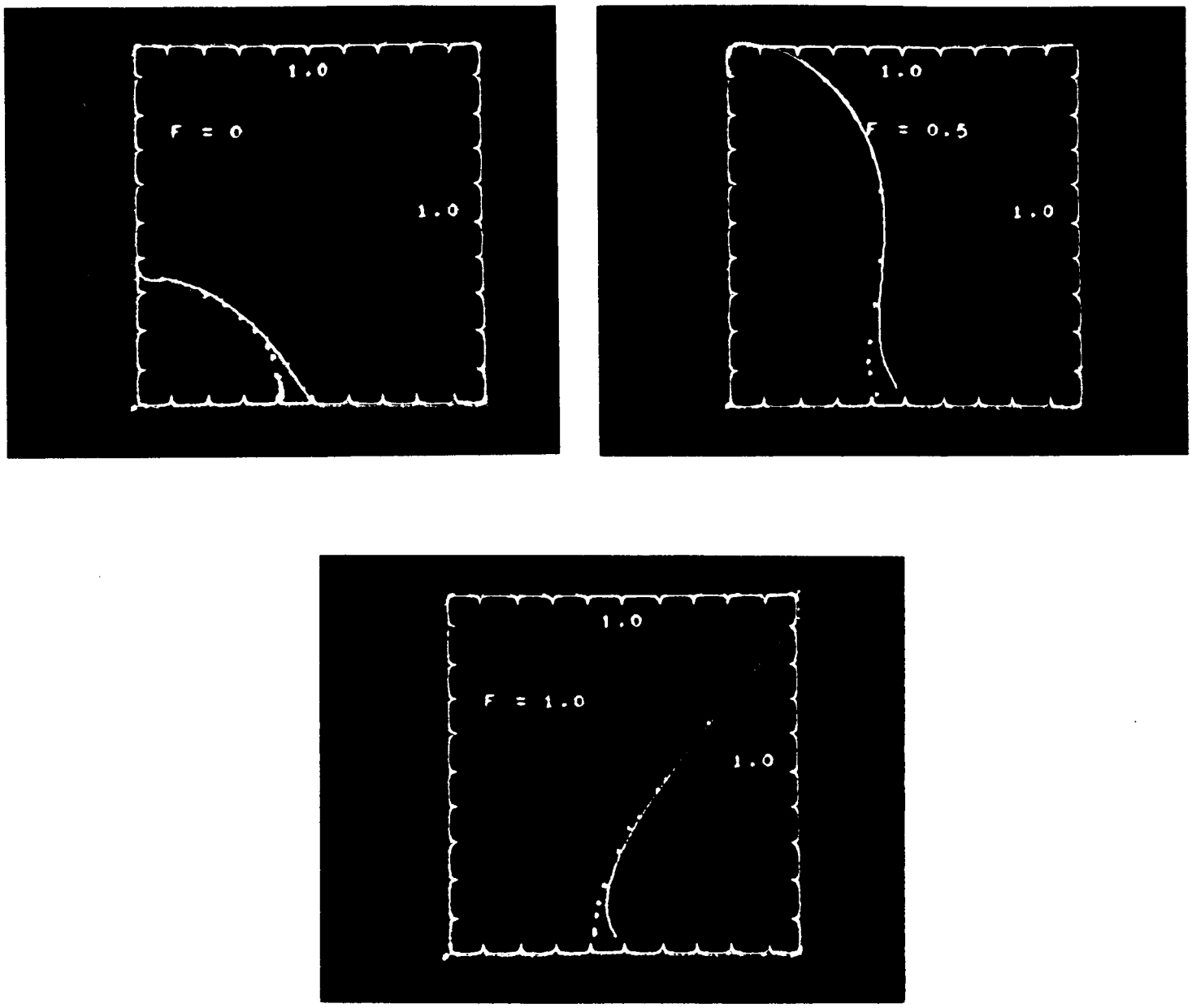

Fig. 9.

Comparison of exact and approximate locii for roots of (7.6) when G is replaced by -G. The heavy dots show the roots obtained using the exact from of G (equation preceeding (7.6)), with various values of E. The solid (or, in the case F = 1.0, the dotted) curve shows the roots obtained using the R-P form (8.5), i.e. the image, under (8.8), of the <u>right-hand</u> branches of Fig. 8.

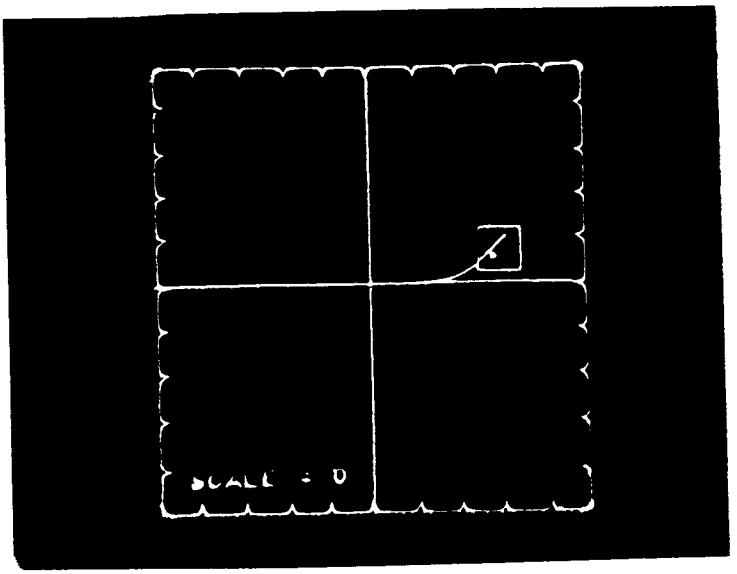

Fig. 10.

Contour, C, in the z plane. Also shown are the R-P contour for this case (F = 0.5) and the value of the root obtained using this square contour in (2.6) with f replaced by G (z) from (7.6) and E = 2.

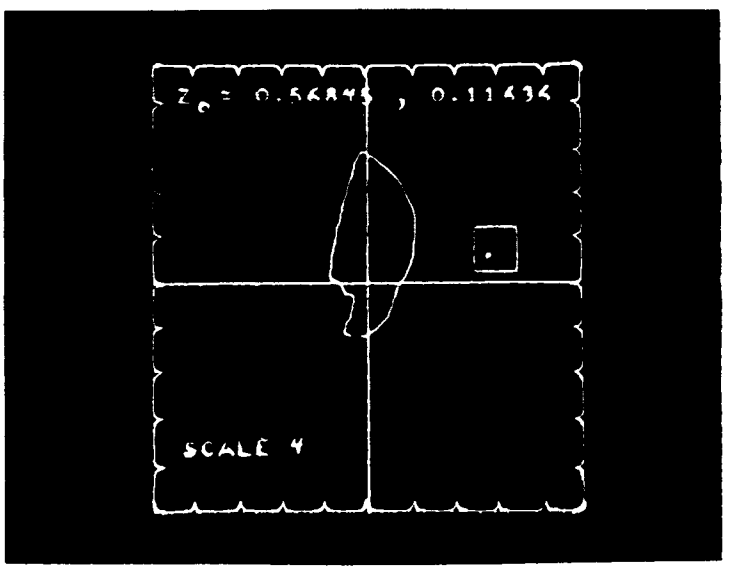

Fig. 11.

Map of the square contour, C, under $z \rightarrow G(z)$. The location and value of the root as given by (2.6) are also shown.

obtaining the value shown in Fig. 11. (This point is shown as a dot in Fig. 10.) To obtain more accuracy we choose z_o as the center of a small circle and use (8.9) to obtain a more accurate value, z_o's, as shown in Fig. 12. This "refinement" process can be repeated as often as desired, but in fact the convergence is extremely rapid (cf Fig. 12).

Of more interest is a sequence of refined root values for varying values of E. Having once computed G(z) (which may require 1 to 2 minutes) for an arc, like that in Fig. 10, which contains roots over some range of E values, for fixed F, we can easily (and quickly!) add F/z^2 to generate H; translate H by subtracting the appropriate E value; and then use (8.9) (with G = H - E in place of H) to find the root. Similarly, for fixed E we can easily find roots as a function of F, for fixed E.

VIII D. Results for the Complex Roots; Variation with Density and Propagation Direction.

Using these methods, we find for the two complex roots identified in VIII A. the behavior shown in Figs. 13 and 14 for several values of E and F. As is to be expected, agreement with the Rosenbluth-Post predictions is better the larger $\mathrm{Im}z_c$, but is nowhere very good since Imz is never larger than about 0.3. Since E is essentially proportional to the reciprocal of density, and $F = \cos^2\theta/\delta$, the dependance of both $\mathrm{Re}\,\omega$ and $\mathrm{Im}\,\omega$ on density and direction of propogation can be inferred directly from these figures.

IX. Discussion of Results

a) We note first that, even for the modest values of Im_z

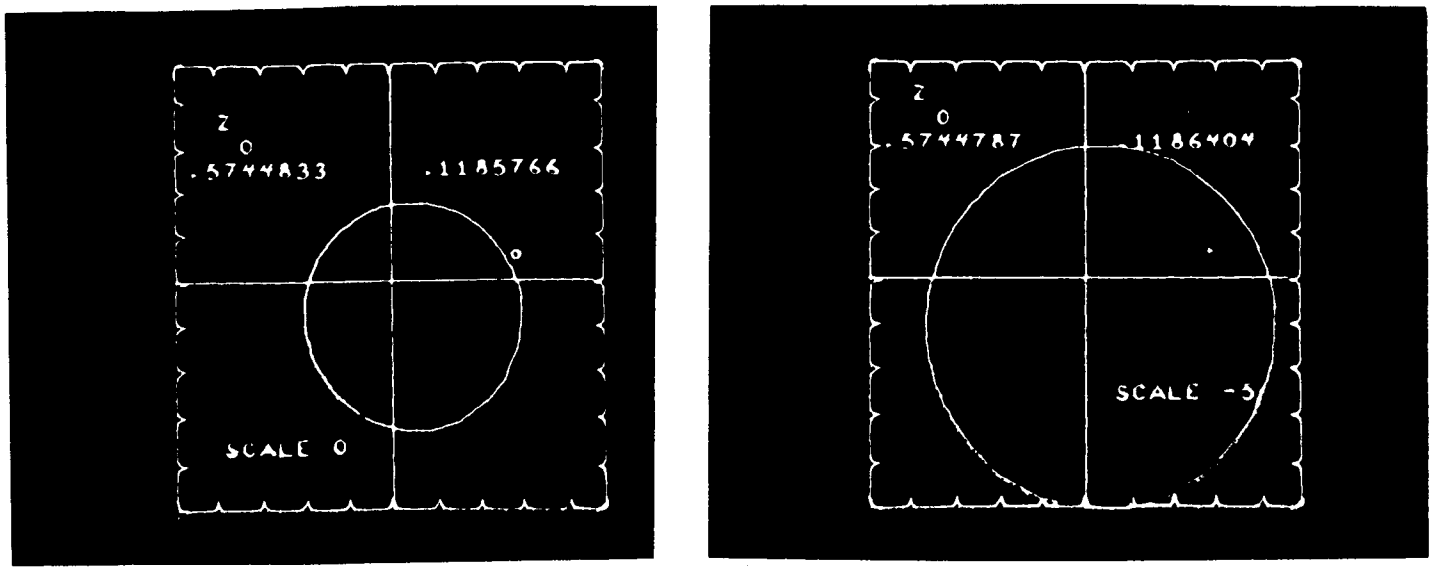

a b

Fig. 12.

Illustration of the refining process

In (a), we see a small circle (radius .02) with center at the approximate root value given in Fig. 11. We also see its map, which is nearly circular and is smaller by a factor 2^{-4} than the map in Fig. 11. The root value found from this new contour is also shown; it differs from the previous value (Fig. 11) by about 1%. In (b) we see the result of one more iteration, resulting from a contour, C, which is a circle of radius .001 about the z_0 value given by (a).

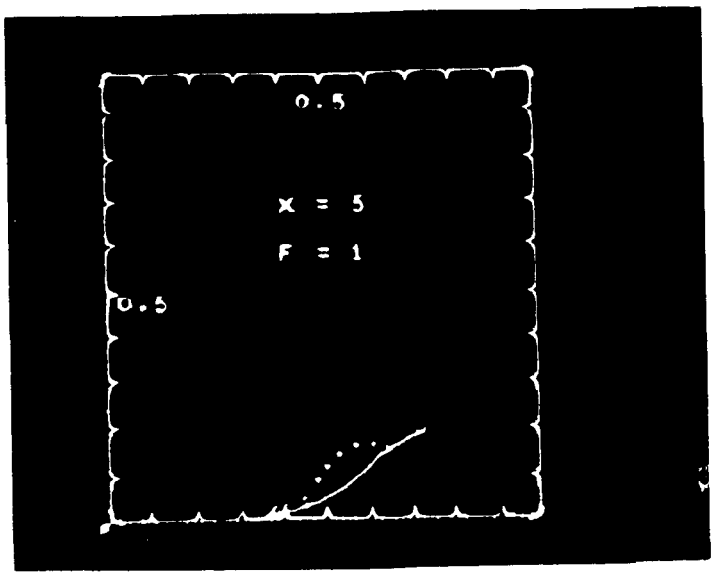

a

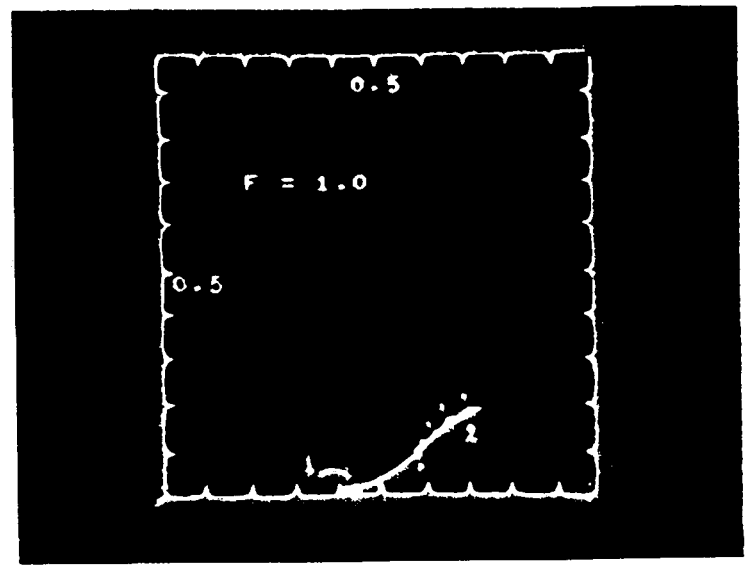

b

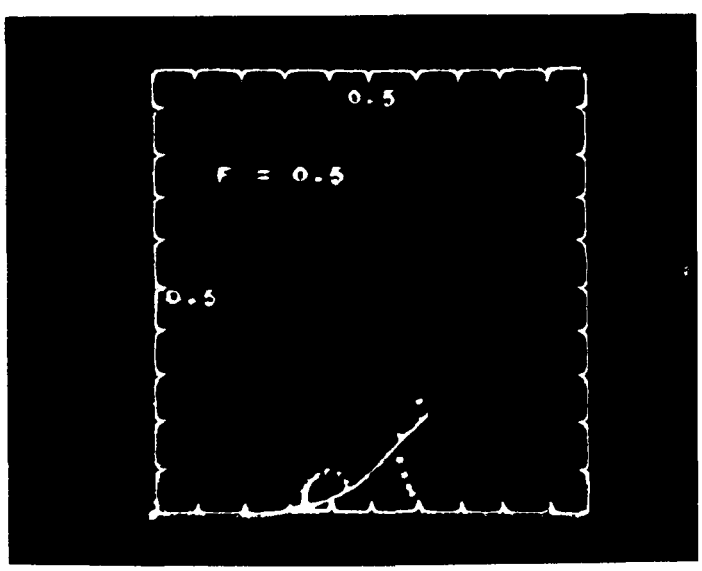

c

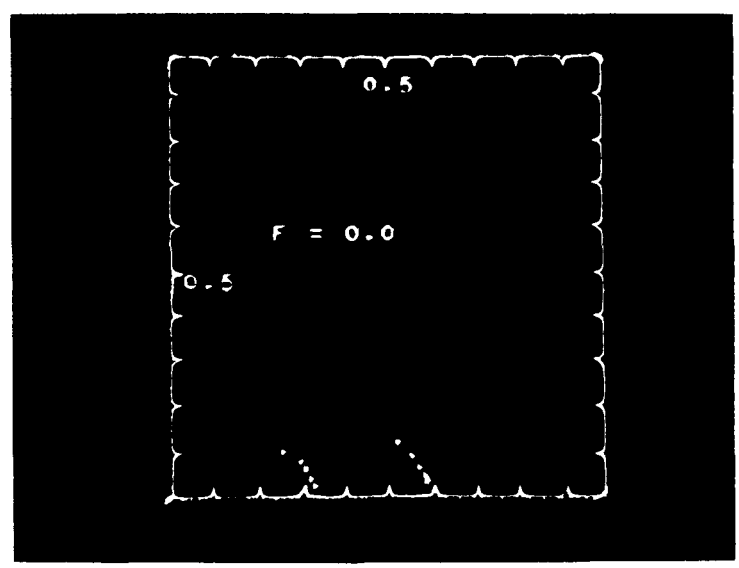

d

Fig. 13.

a) Exact roots for x = 5, F = 1, E = (0, 1, 2, 3, 4, 5, 6, 7, 8, 9) and R-P locus (solid cruve).

b) Same as a) for x = 10; the exact dispersion relation gives two root locii, one shown dotted (E = 0, 1, 2, 3, 4, 5) and the other labelled curve 1. Again, the R-P limit is shown. On both 1 and 2, the point with largest Re z corresponds to E = 0.

c) Same as b), for F = .5. On the right-hand branch. E = (0, 1, 2, 3, 4, 5). On the left-hand branch, E = (0, 1, 2, 3, 4, 5, 6, 7). In both cases, E = 0 is the point with largest Re z. The R-P limit is shown for comparison.

d) Same as c), for F = 0. For the right-hand branch, E = 0, 1, 2, 3, 4; for the left-hand branch, E = 0, .5, 1, 2, 3. In both cases, E = 0 is at the top of the curve.

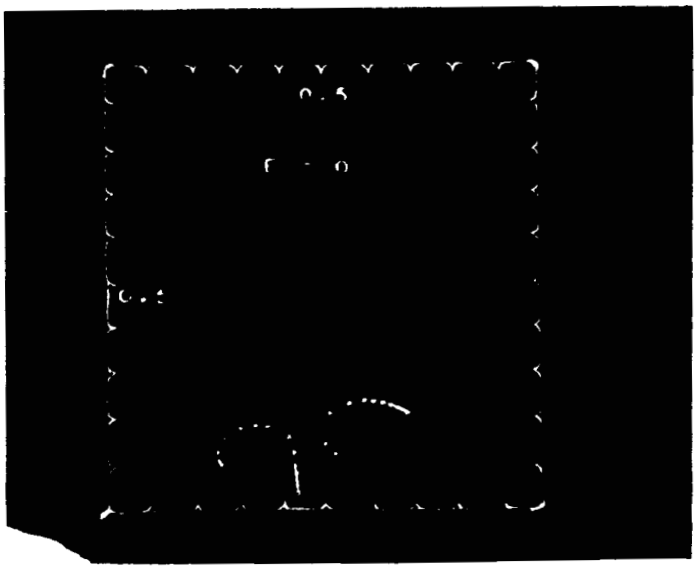

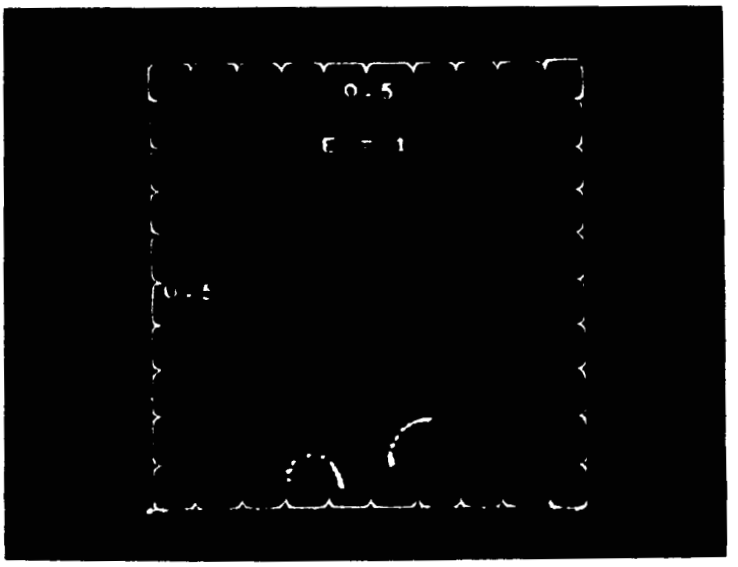

e f

e) Variation of roots with F for fixed E = 0. F ranges from 0 to 1, the right-hand points corresponding to F = 1.

f) Same as e) for E = 1. (E = 0 points are shown as light dots.)

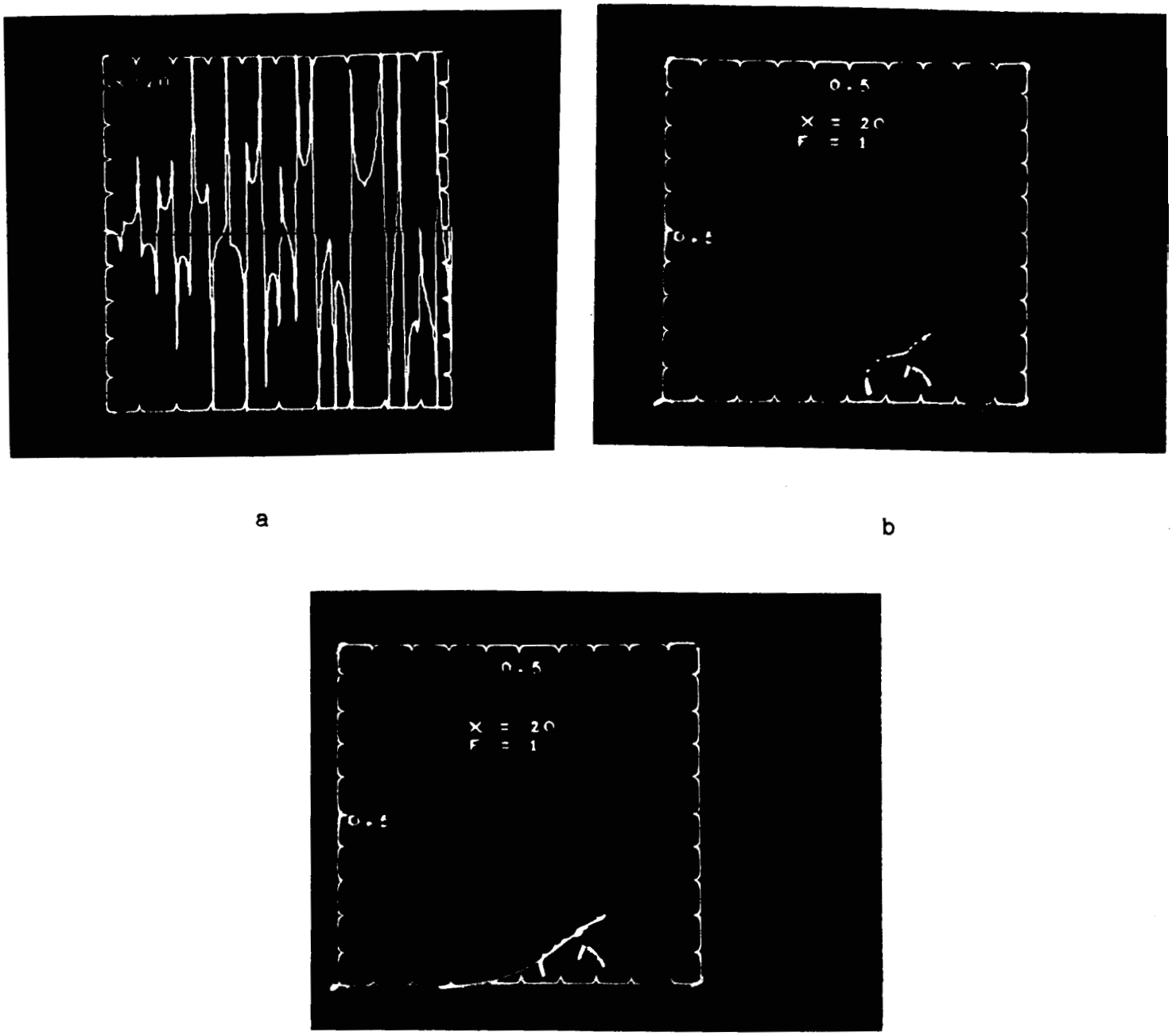

Fig. 14.

Results for the case x = 20.

a) G (z) vs z for real z, $0 \leq z \leq 1$. Each of the six minima corresponds to a branch in the complex z plane.

b) Branches with highest Re z for F = 1, $0 \leq E \leq 10$. In both cases, E = 0 corresponds to the highest Re z.

c) Same as b) with R-P limit shown for comparison.

which we have found, the arguments of the plasma dispersion functions, Z and Z', in (6.3) satisfy

$$\left| \frac{z - n z_c}{\cos\theta \, T_i^{1/2}} \right| >> 1$$

for the range of θ we have used $(0 < \cos^2\theta < \delta)$ and for T_i not too large, e.g. $T_i \sim 1$. Thus, our neglect of ion Landau damping effects is justified.

b) It is clear that the critical parameter involved in the approach to the R-P limit is just the ratio of ion Larmor radius to the wave length. Even for $z_c^{-1} = k R_{ci} = 10$, the agreement between the exact and R-P roots is only indifferently good, and since the latter have maximum Imz of a few tenths, the asymptotic regime $\mathrm{Im}\, z / z_c >> 1$ apparently requires kR_{ci} of order 30 or more.

c) For the range of x considered here $(3 \leq x \leq 20)$, the exact dispersion equation (7.6) has solutions for purely perpendicular propagation (F = 0) with Imω comparable to that found for F = 1, even though the R-P limit predicts that Imω goes to zero with F. (Since the R-P limit is valid only for Imω >> ω_{ci}, it is clear a priori that this latter consequence of the R-P dispersion relation is not reliable.) As we move away slightly from purely perpendicular propagation ($F = 0$), the growth rate increases somewhat and then falls off.

d) While increasing kR_{ci} will, as noted, eventually bring us to the R-P regime, increasing the plasma density (decreasing E) for fixed kR_{ci} will not. For small $kR_{ci} < 10$, the wave is in

resonance with a discrete harmonic of the ion cyclotron motion, the instability drawing its energy from the anisotropy of the ion distribution function, and the R-P limit, which essentially treats R_{ci} as infinite, is a poor approximation.

Investigation of the convective aspects of this instability and the problem of spatial growth are under way.

APPENDIX I

For reference, we provide a list of L_n (x) for x = 10, where

$$\begin{aligned} L_n(x) &\equiv 2n J_n(x) J_n'(x) \\ &= n J_n(x)\left(J_{n-1}(x) - J_{n+1}(x)\right) \\ &= 2n J_n(x)\left(J_{n-1}(x) - \frac{n}{x} J_n(x)\right) \end{aligned} \qquad \text{(A.I.1)}$$

The Bessel functions required were computed by using the recursion relation

$$J_{n-1}(x) = \frac{2n}{x} J_n(x) - J_{n+1}(x) \qquad \text{(A.I.2)}$$

To avoid loss of accuracy the process was initiated at <u>large</u> n and (A.I.2) was used to work down to n = 0. For large initial n = N, an arbitrary <u>positive</u> number (V_N) was chosen and a related set of numbers $V_{N-1}(x), V_{N-2}(x), \ldots,$ $V_0(x)$ computed from (A.I.2). The Bessel functions were then obtained from the normalization

$$1 = \sum_{n=-\infty}^{\infty} J_n^2(x) \approx J_0^2(x) + 2\sum_{n=1}^{N} J_n^2(x) \qquad \text{(A.I.3)}$$

The values of L_n (x) are given in Tables A.1 and A.2.

For larger and larger values of x the dominant terms in the sum in (7.6) occur at larger and larger n ($n \approx x$). We note that asymptotically for large n

$$L_n(n) \approx \frac{1}{\pi^2}\Gamma\left(\frac{1}{3}\right)\Gamma\left(\frac{2}{3}\right) = .368 \tag{A.I.4}$$

independent of n. This is to be compared with $L_{10}(10) = .3501$.

We also list the coefficients

$$K_n = 2J_nJ_n' \qquad n > 0$$

$$K_o = J_oJ_o'$$

needed for the subtracted form (8.2) of $\tilde{G}$.

```
 .
-.217609   - 1
-.75914    - 2
 .830563   - 1
-.2568832
 .2400813
 .39106    - 1
-.5041109
-.1910808
 .2899037
 .3501104
 .1951734
 .715914   - 1
P.1...., LIST OF LN(10).
L0 TO L12.
```

Table A.1. List of L_n (10) $\equiv 2nJ_n$ (10) J_n' (10) for n = 0 to 12.

```
 .3501104
 .1951734
 .715914   - 1
 .19364    - 1
 .40952    - 2
 .7025     - 3
 .1003     - 3
 .12       - 4
 .11       - 5
 (
 (
 (
 (
P.2...., LIST OF LN(10).
L10 TOL18.
```

Table A.2. Continued list of L_n (10); n = 10 to 18.

N	$K_N = 2J_N J'_N$	
0	.1069146	-1
1	-.217609	-1
2	-.3795743	-2
3	.2768546	-1
4	-.642208	-1
5	.4801623	-1
6	.6517693	-2
7	-.7201582	-1
8	-.2388511	-1
9	.322115	-1
10	+1 .3501103	-1
11	.1774305	-1
12	.5965956	-2
13	.1489542	-2
14	.292521	-3
15	.4683807	-4
16	.6269664	-5
17	.7115304	-6
18	.6705523	-7
19	.3725390	-8
20	+1 0	

Table A.3. List of K_n (10) $\equiv 2\ J_n J'_n$ $(n \geq 1)$ vs n.

REFERENCES

1. McCune, J. E., Phys. Flu., 9, 10, 2082, (1966).

2. Fried, B. D., "On-Line Root Finding in the Complex Plane", Report No. 9990-7308-R0000, Physical Research Center, TRW Systems, Redondo Beach, Calif., July (1966).

3. "Man-Computer Systems", W. Karplus, ed., Chapter 5, "On-Line Problem Solving" by B. D. Fried and Appendix (User's Manual for UCSB On-Line System) by G. Culler, McGraw-Hill (in press). B. D. Fried, "STL On-Line Computer", Vol. I, C. C. Farrington and D. Pope, "Users Manual", Vol. II, TRW Systems Report 9824-6001-RU-000, Dec. (1964).

4. Knopp, K., "Theory of Functions", Dover Publications, New York (1945).

5. Harris, E. G., J. Nucl. En., Part C: Plasma Physics, 2, 138 (1961).

6. Rosenbluth, M. N. and Post, R. F., Phys. Flu. 8, 3, 547 (1965).

7. Dory, R. A., Guest, G. E., Harris, E. G., Phys. Rev. Letters 14, 5, 131 (1965).

8. Guest, G. E. and Dory, R. A., Phys. Fluids, 8, 10, 1853 (1965).

9. Fried, B. D. and Conte, S. D., "The Plasma Dispersion Function", Academic Press, New York (1961).

10. "Plasma Physics, Lectures presented at a Seminar, Trieste", Chapter entitled "Microinstabilities" by M. N. Rosenbluth, International Atomic Energy Agency, Vienna (1965).